Atomic-level mechanism of elastic deformation in the Zr-Cu metallic glass

J. Antonowicz* and A. Pietnoczka
Faculty of Physics, Warsaw University of Technology, Koszykowa 75, 00-662 Warsaw, Poland

G. A. Evangelakis
Department of Physics, University of Ioannina, Ioannina 45110, Greece

O. Mathon, I. Kantor,† and S. Pascarelli
European Synchrotron Radiation Facility, F-38043 Grenoble, France

A. Kartouzian
Chemistry Department, Catalysis Research Center, Technical University of Munich, Lichtenbergstraße 4, 85748 Garching, Germany

T. Shinmei and T. Irifune
Geodynamics Research Center, Ehime University, 2-5 Bunkyo-cho, Matsuyama 790-8577, Japan
(Received 19 May 2015; revised manuscript received 20 March 2016; published 15 April 2016)

To explore the microscopic response of a metallic glass (MG) to an applied hydrostatic load we performed a high-pressure extended x-ray absorption fine structure (EXAFS) study of the $Zr_{66.7}Cu_{33.3}$ amorphous alloy. EXAFS fitting revealed that on compression, Zr-Zr pairs are strained preferentially. Strong Zr-Cu interactions contribute to the stiffness of dominant Cu-centered clusters and the overall compressibility of the MG is mostly determined by the softer bonds between the Zr atoms belonging to the clusters' outer shell. Stress accommodation is accompanied by a variation of bonding preferences, which is consistent with the observed hierarchy of elastic constants of different atomic pairs.

DOI: 10.1103/PhysRevB.93.144115

The superior mechanical properties of metallic glasses (MGs) are commonly attributed to their disordered atomic structure described in terms of efficiently packed clusters of atoms [1]. In particular, the elastic limit of $\sim$2% makes MGs promising candidates for a wide range of structural applications. Despite numerous efforts towards understanding the microscopic mechanism of elastic deformation in MGs, very little is known about the actual response of their nonperiodic atomic arrangement to the applied stress and the knowledge relies mainly on simulations. The elasticity of MGs is determined by complex interactions between different atomic species within tightly bound clusters as well as bonding characteristics of intercluster junctions. For this reason, unlike in crystalline solids, elastic deformation of MGs is intrinsically inhomogeneous. Previous studies have revealed that elastic deformation of MGs depends on the length scale so that nearest-neighbor shells are stiffer than more distant shells [2–6]. The inhomogeneous nature of MGs is reflected in nanoscale variations of elastic modulus [7] and viscoelasticity [8] identified by atomic force microscopy. Recently, Ma *et al.* [9] showed that MGs inherit their elastic properties from their solvent atoms [10] suggesting rubberlike viscoelastic behavior of MGs. Molecular dynamics simulations of binary Cu-Zr MGs concluded that Cu-centered icosahedral clusters are resistant to elastic [11] and plastic [12] deformation.

Extended x-ray absorption fine structure (EXAFS) is a powerful experimental technique highly sensitive to local atomic order around selected atomic species [13]. As such, EXAFS is a particularly useful method for resolving the atomic-level structure in disordered materials such as MGs [14–16]. In this work we employ EXAFS analysis to follow the microstructural evolution under applied hydrostatic load in a binary $Zr_{66.7}Cu_{33.3}$ MG. We show that hydrostatic stress is mostly accommodated by straining Zr-Zr bonds, while strong Zr-Cu interactions contribute to the stiffness of dominant Cu-centered clusters. The hierarchy of stiffness among atomic pairs underlies the variation of bonding preferences favoring like-atom bonds at elevated pressure.

The EXAFS experiments at the Cu K edge (8979 eV) and Zr K edge (17998 eV) were carried out in transmission at the BM23 beamline of the European Synchrotron Radiation Facility [17]. High-pressure EXAFS measurements were performed using a mechanical piston-cylinder diamond anvil cell [18]. To avoid unwanted signal distortions of EXAFS spectra we used recently developed sintered nanopolycrystalline diamond (NPD) anvils [19]. These diamond anvils are clear and transparent and provide clean glitch-free EXAFS spectra in any energy range [20]. The background absorption due to the high pressure cell (two 1.5-mm diamond anvils) was 97% and 40% at the Cu and Zr K edges, respectively. Harmonic rejection was achieved by means of two Pt-coated silicon mirrors at grazing incidence angles of 6 and 3.5 mrad at the Cu and Zr K edges, respectively, leading to efficient harmonic rejection: the third harmonic is suppressed by a factor 3.7×10^{-5} and 8.6×10^{-6} at the Cu and Zr K edges, respectively, with respect to the intensity of the fundamental. Two 50-mm-long ion chambers operating at 1000 V were utilized to measure the incoming (I_0) and transmitted (I_1) flux. The choice of gas and the pressure in the chambers were

*antonowi@if.pw.edu.pl
†Current address: Technical University of Denmark, Fysikvej 307, 2800 Kgs. Lyngby, Denmark.

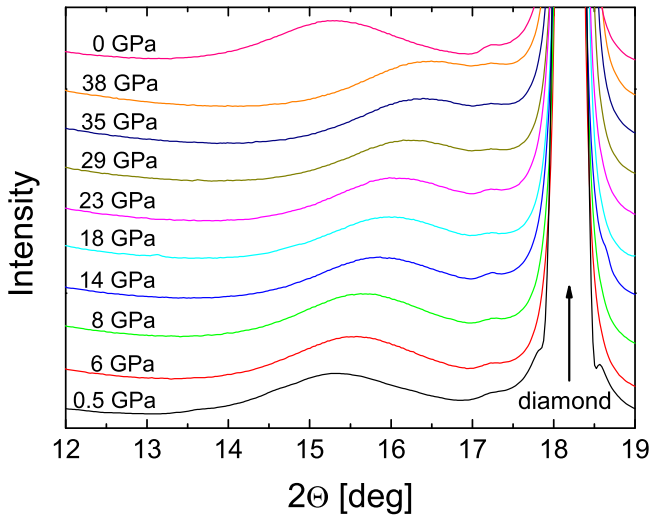

FIG. 1. Pressure-dependent XRD spectra for $Zr_{66.7}Cu_{33.3}$ MG. Strong Bragg peak located at $2\theta = 18.2^{\circ}$ originates from the NPD anvil.

optimized to have a 30% (I_0) and 70% (I_1) absorption. Argon (0.7 bar for I_0 and 2 bars for I_1) and Krypton (0.3 bar for I_0 and 1.0 bar for I_1) were used at the Cu and Zr K edges, respectively. Helium was added (when necessary) to reach a final pressure of 2 bars in both chambers.

The x-ray diffraction (XRD) spectra taken during compression ramp up to 38 GPa together with the spectrum taken after decompression to equilibrium pressure are shown in Fig. 1. The diffraction patterns were collected in transmission through NPD anvils and thus the spectra are dominated by the strong (111) Bragg peak of diamond. Under load, a diffuse diffraction maximum originating from the glassy sample shifts progressively to higher angles and reflects a decrease of the average interatomic distance. Judging from the XRD data the deformation under applied hydrostatic stress is fully reversible and the amorphous character of the sample is maintained over the whole pressure range.

Figure 2 shows the Zr K-edge and Cu K-edge k^2-weighted $\chi(k)$ oscillations (here referred to as "the EXAFS") and magnitude of their Fourier transform (FT) at different pressure values. Apparently, the amplitude of EXAFS is approximately 40% higher for the Cu than for the Zr edge. This simple observation carries important information on the degree of short-range order (SRO) around Cu and Zr atoms. Since the measured EXAFS is an average of $\chi(k)$ functions of all the absorbing atoms in the irradiated volume, the degree of regularity in local atomic arrangement around the absorbing species is proportional to the amplitude of the corresponding EXAFS. In the present case of the binary Zr-Cu MG the difference in EXAFS amplitude is experimental evidence of the prevalence of SRO around Cu atoms. In the cluster description, Cu acts mostly as the core atom of the constituent clusters with Zr atoms located preferentially in the first-neighbor shell (FNS) of Cu-centered clusters. FT EXAFS shown in Fig. 2 exhibits a split peak corresponding to Cu-Cu and Cu-Zr pairs in the case of the Cu-edge and Zr-Cu and Zr-Zr pairs in the case of Zr-edge spectra. The apparent pressure dependence of the EXAFS signal represents the microscopic response of the MG to applied hydrostatic load. To extract quantitative structural information from the absorption data, we have carried out nonlinear EXAFS fitting resulting in partial coordination numbers, interatomic distances, and their distribution in FNS for Cu and Zr absorption edge spectra. We note that as both XRD and EXAFS spectra fully recover after compression and subsequent decompression with no indication of hysteresis, we do not distinguish between spectra taken during compression and decompression ramps throughout this paper.

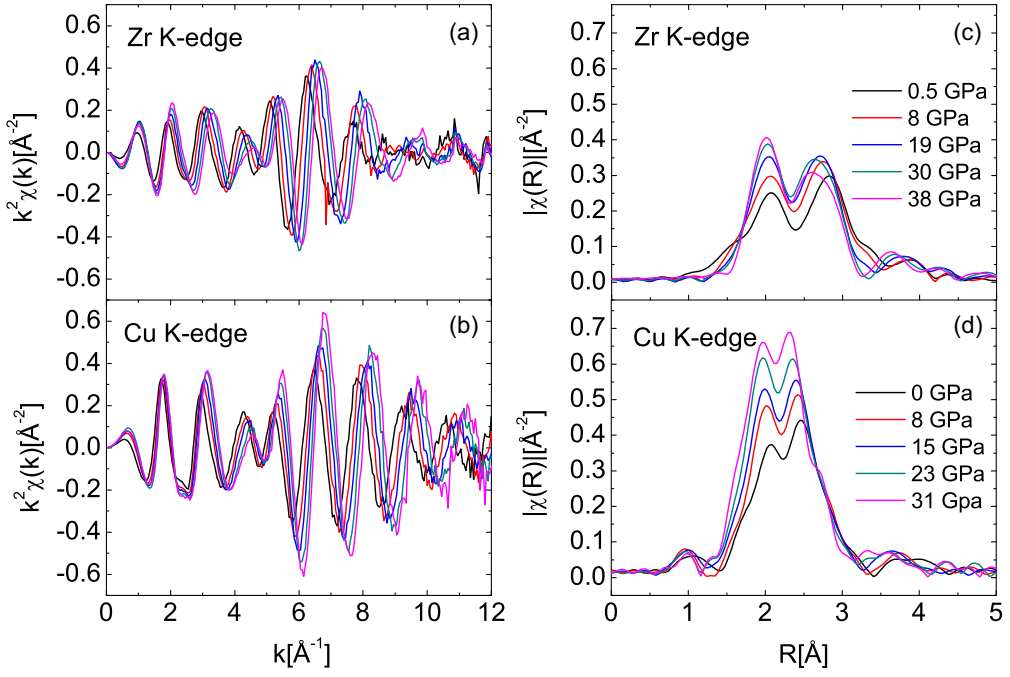

FIG. 2. Zr K edge and Cu K edge k^2-weighted EXAFS oscillations [(a),(b)] and magnitude of their Fourier transforms [(c),(d)] at different pressure values.

To analyze the absorption data we applied a multiparameter fitting technique using the ARTEMIS code [21]. The EXAFS oscillations formula for a single shell is given by [22]

$$\chi(k) = \frac{NS_0^2}{kR^2}|f^{\text{eff}}(k)|e^{-2\sigma^2k^2}\sin[2kR + \delta(k)], \qquad (1)$$

where R is the interatomic distance, N is the number of nearest-neighbor atoms (coordination number), S_0^2 is the amplitude reduction factor, f^{eff} is the photoelectron effective scattering amplitude, σ^2 is mean-square relative displacement (MSRD) in the interatomic distance (Debye-Waller factor), δ is the photoelectron phase shift, and k is the photoelectron wave number.

In the present study, we treated S_0^2 as a phenomenological parameter that accounts for any k-independent suppression of $\chi(k)$ oscillations [23]. In such approach S_0^2 does not have any particular physical meaning but accounts for all experimental effects (errors in data normalization, detector nonlinear response, sample inhomogeneity) and theoretical limitations (errors in FEFF 's model) that systematically affect EXAFS amplitude. The values of $S_0^2 = 0.40$ for Cu and $S_0^2 = 0.44$ for Zr were determined by back-calculation to obtain total coordination numbers $N_{\text{Cu-Zr}} + N_{\text{Cu-Cu}}$=11 and $N_{\text{Zr-Zr}} + N_{\text{Zr-Cu}}$=14 (Zr-Cu and Cu-Zr indexes denote the values for the Zr edge and Cu edge, respectively). Those values are maximal coordination numbers allowed by topology in a hard-sphere approximation assuming Goldschmidt radii of atoms. A range of Cu and Zr coordination numbers has been reported in the literature [24–26] and our current assumption on maximal local packing density of atoms may slightly overestimate the actual values. According to our estimations, the uncertainty of coordination numbers does not exceed 10%. Since S_0^2, N, and MSRD are highly correlated [22], the arbitrary assumption of N induces a systematic error of the MSRD. The estimated uncertainty of MSRD is 10%. We note that in our study we do not put emphasis on the absolute values of total coordination numbers and MSRDs and our conclusions are based on the pressure dependencies of R, N, and σ^2. Further details of the EXAFS fitting procedure are given in the Supplemental Material [27].

During hydrostatic compression of the MG, different types of atomic pairs are strained to accommodate the applied stress. If no structural phase transition occurs on compression, fractional volume reduction V/V_0 (where V_0 is volume at zero pressure) is proportional to atomic spacing cubed. The relationship between volume (or atomic spacing) change and applied hydrostatic pressure can be described in terms of an isothermal equation of state (EOS) involving bulk modulus B, which is the measure of materials resistance to compression. Our combined XRD/EXAFS approach allowed us to access both mean atomic spacing of the amorphous structure as well as specific types of bond distances (Zr-Zr, Cu-Cu, Cu-Zr). The mean atomic spacing in the amorphous solid scales with $1/q_m$ where q_m is the q position of the first XRD intensity maximum and $q = 4\pi \sin\theta/\lambda$ (where θ is half of the scattering angle and λ is the x-ray wavelength) [28]. On the other hand, specific interatomic distances: $R_{\text{Zr-Zr}}$, $R_{\text{Cu-Cu}}$, $R_{\text{Cu-Zr}}$, and $R_{\text{Zr-Cu}}$ are obtained by EXAFS fitting. While the shift of q_m represents actual volume shrinkage of the sample, the variation of specific bond distances R cannot be readily related to any macroscopic volume change. Still, relative bond distance shortening can be used as an argument of the EOS function to evaluate compressibility of the bond.

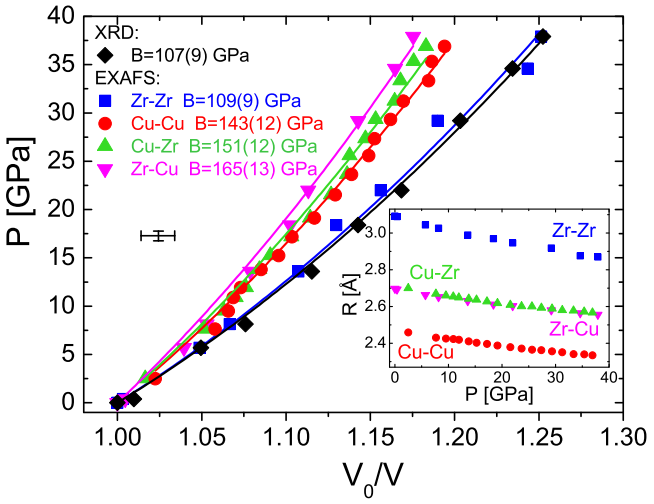

FIG. 3. The results of Birch-Murnaghan EOS fitting to XRD and EXAFS data (cross indicates error bars). The evolution of interatomic distances derived from EXAFS fitting is shown in the inset. The error bars of R are smaller than symbols.

To relate interatomic pair distances R and diffraction peak position q_m to the applied pressure we employed a second-order Birch-Murnaghan EOS [29] $P(V) = 3B/2[(V_0/V)^{7/3} - (V_0/V)^{5/3}]$ replacing V_0/V with $(R_0/R)^3$ and $(q/q_{m0})^3$ (where R_0 and q_{m0} refer to values at zero pressure). The results of the EOS fitting to the XRD and EXAFS data are presented in Fig. 3 and the evolution of the interatomic distances derived from EXAFS is shown in the inset. We note that independent fitting of the Cu and Zr-edge spectra yields $R_{\text{Cu-Zr}}$ and $R_{\text{Zr-Cu}}$ overlapping within error bars of 0.01 Å (0.4%) which proves that the current EXAFS analysis is meaningful and consistent since these two parameters represent the same physical quantity. The fitted values of interatomic distances are in accordance with previously published reverse Monte Carlo [26], EXAFS [30], and XRD [24,25,31] data on Cu-Zr MGs. The value of bulk modulus of $B = 107(9)$ GPa derived from the shift of the diffraction maximum is in good agreement with that reported in the literature data based on macroscopic measurements for closely related amorphous alloys [32]. Furthermore, a sequence of $P(V)$ functions derived from EXAFS data illustrates a hierarchy of stiffness of different atomic pairs. On compression, Zr-Zr distances are strained preferentially [$B = 109(9)$ GPa], while Cu-Cu pairs appear stiffer [$B = 143(12)$ GPa]. The unlike atom pairs are most resistant to the applied load: 151(12) and 165(13) GPa for Cu-Zr and Zr-Cu, respectively. For the like-atom interaction, the values of bulk modulus are close to those characteristic for the pure, crystalline state (91 GPa for zirconium and 140 GPa for copper). Due to high sensitivity to small variations of R the uncertainties of B reach 8%, nevertheless the bulk moduli obtained independently from Cu and Zr-edge measurements overlap within uncertainty range.

The presence of a hierarchy of stiffness of different atomic pairs sheds some light on the atomic-level mechanism of elastic deformation of the glassy alloy. As deduced from the difference in Cu and Zr EXAFS amplitude (Fig. 2), Cu-centered clusters dominate the atomic structure of the amorphous alloy. It follows that stiff Cu-Zr pairs correspond mainly to core-shell interactions within the cluster, while soft Zr-Zr (shell-shell) bonds are mostly responsible for linking between clusters. Since, due to alloy stoichiometry, the number of bonds of Zr-Zr highly exceeds that of Cu-Zr and Cu-Cu, the overall elasticity of the MG is mostly determined by interactions between Zr atoms, which is manifested by the fact that the bulk modulus of $Zr_{66.7}Cu_{33.3}$ glass and Zr-Zr atomic pairs in that glass are nearly equal. This conclusion is consistent with recent observations of Ma *et al.* [9] and Wang [10] concerning inheritance of elastic properties of the MGs from their solvent atoms. Furthermore, it is in agreement with previously published works reporting on nonhomogeneous deformation of MGs and demonstrating that short-range order of the MG is less sensitive to stress than medium-range order [3].

Besides interatomic distances, the information on the number and type of absorber neighbors is encoded in EXAFS oscillations. To satisfy fundamental constraints on the atomic pair distribution function resulting from alloy stoichiometry, we imposed constraints on the fitted partial coordination numbers, thus limiting the number of unknown parameters in the fit. Namely, we approximated the pressure dependence of $N_{\text{Cu-Zr}}$ with a linear function and set $N_{\text{Zr-Cu}}$ to be equal to $N_{\text{Cu-Zr}}(P)/2$. Since total coordination numbers of Cu and Zr were fixed, the like-atom partial coordination numbers $N_{\text{Cu-Cu}}$ and $N_{\text{Zr-Zr}}$ were not independent fitting parameters. Figure 4(a) presents the evolution of partial coordination numbers of Cu and Zr atoms derived from EXAFS fitting together with the linear fit to $N_{\text{Cu-Zr}}(P)$ data. The equilibrium pressure results closely match the partial coordination numbers derived from XRD data by Mattern *et al.* [25] and show small deviations from values given in Refs. [24,26,30] for the Zr-rich amorphous Cu-Zr alloys. The current high-pressure data show a progressive decrease of unlike-atom pairs (also observed in semiconductors [33]) at the expense of like-atom pairs providing evidence of a rearrangement in the SRO occurring on compression. This observation is in line with previous reports on the nonaffine character of elastic deformation of MGs [11] and highlights a complex interplay between mechanical response and the details of the atomic arrangement of glassy metals. A coherent description of the atomic-scale deformation mechanism requires that pressure dependencies of bond distances and partial coordination numbers are correlated. Indeed, the observed variation of bonding preferences is consistent with the hierarchy of stiffness of different atomic pairs. As Zr-Zr and Cu-Cu distances are more easily strained than Zr-Cu, one should expect that the contribution of like-atom nearest neighbors increases on structure densification, as observed in Fig. 4(a).

Pressure-induced rearrangement in the SRO was found to be assisted by variations of disorder parameter σ^2. In our fits, MSRDs for different pair types were treated as free fitting parameters. To account for a well known effect of the correlation between MSRD and coordination number we applied a decorrelation procedure to obtain a unique set

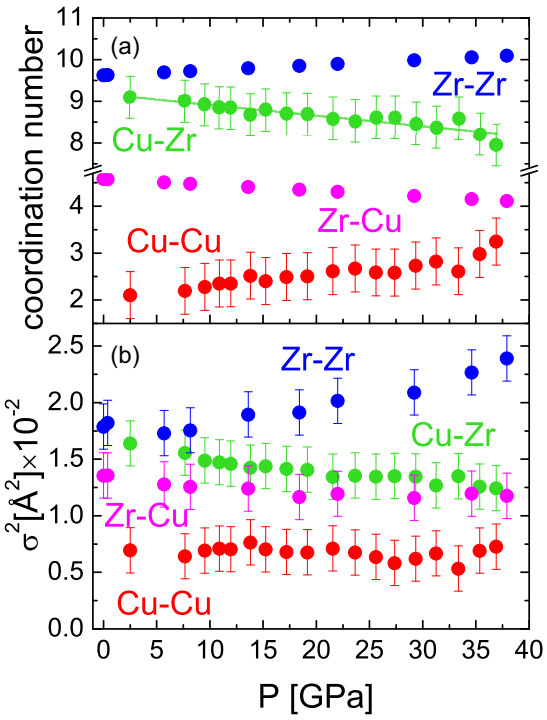

FIG. 4. Partial coordination numbers (a) and Debye-Waller factors (b) as a function of applied pressure. The solid line represents linear fit to $N_{\text{Cu-Zr}}$ data points.

of parameters. The fitted pressure dependencies of σ^2 are presented in Fig. 4(b). While MSRDs exhibit relatively large uncertainties, the independently fitted values of $\sigma^2_{\text{Cu-Zr}}$ and $\sigma^2_{\text{Zr-Cu}}$, which represent the same physical quantity, overlap within error bars and show a decreasing trend. On the other hand, $\sigma^2_{\text{Cu-Cu}}$ remains approximately constant on compression and its value is clearly lower than for Cu-Zr/Zr-Cu. Finally, MSRD for Zr-Zr pairs is apparently the highest of all and the value of $\sigma^2_{\text{Zr-Zr}}$ grows with increasing pressure. The high degree of structural disorder around Zr as compared to Cu atoms is reflected by stronger damping of the Zr-edge EXAFS oscillations as seen clearly in the raw data shown in Fig. 2. Judging from the results on MSRDs, the amorphous structure is organized around Cu rather than Zr atoms. In terms of atomic clusters, the amorphous structure involves clusters formed preferentially around Cu [11,12,34]. The elastic compression is associated with the ordering of Cu-Zr and disordering of Zr-Zr pair distances. In accordance with our interpretation of the R and N pressure dependencies, strong bonds between clusters' central (Cu) and shell atoms (Zr) form a stiff backbone which tends to become more ordered with increasing pressure. Elastic deformation of the amorphous structure is mostly accomplished by straining of soft Zr-Zr (shell-shell) pairs. To accommodate the applied stress, the contribution of those pairs increases and Zr-Zr bond distance distribution becomes broader.

In summary, by means of high-pressure EXAFS the atomic-level mechanism of elastic deformation of the $Zr_{66.7}Cu_{33.3}$ MG has been revealed in detail. A simple comparison of oscillation amplitudes of Cu and Zr-edge EXAFS provides evidence of the prevalence of Cu-centered clusters. The EXAFS fitting

results indicate that during hydrostatic loading the stress accommodation is not uniform. As pressure increases, Zr-Zr pairs are strained preferentially, while distances between the clusters' central (Cu) and shell atoms (Zr) remain least affected by the external load. The nonuniform structural deformation is accompanied by the variation of bonding preferences. With increasing pressure, the contribution of like-atom pairs increases at the expense of unlike-atom bonds, which is consistent with the observed hierarchy of stiffness of different atomic pairs. In the process of stress accommodation, the core-shell (Cu-Zr) bond distance distribution becomes narrower, while that of the shell-shell (Zr-Zr) pairs gets broader. This work confirms earlier suggestions that elastic deformation of MGs is intrinsically inhomogeneous. The conclusion on strongly bound, stiff, Cu-centered clusters is in agreement with previously published results on the deformation mechanism of Cu-Zr amorphous alloys.

We acknowledge the European Synchrotron Radiation Facility for the provision of synchrotron radiation facilities.

[1] A. Yavari, Nature (London) **439**, 405 (2006).
[2] H. Poulsen, J. Wert, J. Neuefeind, V. Honkimäki, and M. Daymond, Nat. Mater. **4**, 33 (2005).
[3] T. C. Hufnagel, R. T. Ott, and J. Almer, Phys. Rev. B **73**, 064204 (2006).
[4] W. Dmowski, T. Iwashita, C.-P. Chuang, J. Almer, and T. Egami, Phys. Rev. Lett. **105**, 205502 (2010).
[5] J. Plummer and I. Todd, Philos. Mag. **92**, 2894 (2012).
[6] U. K. Vempati, P. K. Valavala, M. L. Falk, J. Almer, and T. C. Hufnagel, Phys. Rev. B **85**, 214201 (2012).
[7] H. Wagner, D. Bedorf, S. Kchemann, M. Schwabe, B. Zhang, W. Arnold, and K. Samwer, Nat. Mater. **10**, 439 (2011).
[8] Y. H. Liu, D. Wang, K. Nakajima, W. Zhang, A. Hirata, T. Nishi, A. Inoue, and M. W. Chen, Phys. Rev. Lett. **106**, 125504 (2011).
[9] D. Ma, A. D. Stoica, X.-L. Wang, Z. P. Lu, B. Clausen, and D. W. Brown, Phys. Rev. Lett. **108**, 085501 (2012).
[10] W. H. Wang, Nat. Mater. **11**, 275 (2012).
[11] J. Ding, Y. Q. Cheng, and E. Ma, Appl. Phys. Lett. **101**, 121917 (2012).
[12] C. E. Lekka, A. Ibenskas, A. R. Yavari, and G. A. Evangelakis, Appl. Phys. Lett. **91**, 214103 (2007).
[13] J. J. Rehr and R. C. Albers, Rev. Mod. Phys. **72**, 621 (2000).
[14] K. Saksl, H. Franz, P. Jovari, K. Klementiev, E. Welter, A. Ehnes, J. Saida, A. Inoue, and J. Z. Jiang, Appl. Phys. Lett. **83**, 3924 (2003).
[15] J. Antonowicz, A. Pietnoczka, W. Zalewski, R. Bacewicz, M. Stoica, K. Georgarakis, and A. Yavari, J. Alloys Compd. **509**, S34 (2011).
[16] W. Zalewski, J. Antonowicz, R. Bacewicz, and J. Latuch, J. Alloys Compd. **468**, 40 (2009).
[17] O. Mathon, A. Beteva, J. Borrel, D. Bugnazet, S. Gatla, R. Hino, I. Kantor, T. Mairs, M. Munoz, S. Pasternak, F. Perrin, and S. Pascarelli, J. Synchrotron Radiat. **22**, 1548 (2015).
[18] I. Kantor, V. Prakapenka, A. Kantor, P. Dera, A. Kurnosov, S. Sinogeikin, N. Dubrovinskaia, and L. Dubrovinsky, Rev. Sci. Instrum. **83**, 125102 (2012).
[19] T. Irifune, A. Kurio, S. Sakamoto, T. Inoue, and H. Sumiya, Nature (London) **421**, 599 (2003).
[20] N. Ishimatsu, K. Matsumoto, H. Maruyama, N. Kawamura, M. Mizumaki, H. Sumiya, and T. Irifune, J. Synchrotron Radiat. **19**, 768 (2012).
[21] M. Newville, J. Synchrotron Radiat. **8**, 322 (2001).
[22] G. Bunker, *Introduction to XAFS: A Practical Guide to X-ray Absorption Fine Structure Spectroscopy* (Cambridge University Press, Cambridge, UK, 2010).
[23] S. Calvin, *XAFS for Everyone* (CRC Press, Boca Raton, FL, 2013).
[24] H. Chen and Y. Waseda, Phys. Status Solidi A **51**, 593 (1979).
[25] N. Mattern, A. Schöps, U. Kühn, J. Acker, O. Khvostikova, and J. Eckert, J. Non-Cryst. Solids **354**, 1054 (2008).
[26] N. Mattern, P. Jóvári, I. Kaban, S. Gruner, A. Elsner, V. Kokotin, H. Franz, B. Beuneu, and J. Eckert, J. Alloys Compd. **485**, 163 (2009).
[27] See Supplemental Material at http://link.aps.org/supplemental/10.1103/PhysRevB.93.144115 for a detailed description of sample preparation, high-pressure X-ray absorption experiment and EXAFS fitting procedure.
[28] A. Guinier, *X-ray Diffraction* (W.H. Freeman and Co., New York, 1963).
[29] F. Birch, J. Geophys. Res. **57**, 227 (1952).
[30] L. Yang, J. H. Xia, Q. Wang, C. Dong, L. Y. Chen, X. Ou, J. F. Liu, J. Z. Jiang, K. Klementiev, K. Saksl, H. Franz, J. R. Schneider, and L. Gerward, Appl. Phys. Lett. **88**, 241913 (2006).
[31] K. Georgarakis, A. Yavari, D. Louzguine-Luzgin, J. Antonowicz, M. Stoica, Y. Li, M. Satta, A. LeMoulec, G. Vaughan, and A. Inoue, Appl. Phys. Lett. **94**, 191912 (2009).
[32] W. H. Wang, Prog. Mater. Sci. **57**, 487 (2012).
[33] G. Aquilanti and S. Pascarelli, J. Phys.: Condens. Matter **17**, 1811 (2005).
[34] J. Antonowicz, A. Pietnoczka, T. Drobiazg, G. A. Almyras, D. G. Papageorgiou, and G. A. Evangelakis, Philos. Mag. A **92**, 1865 (2012).